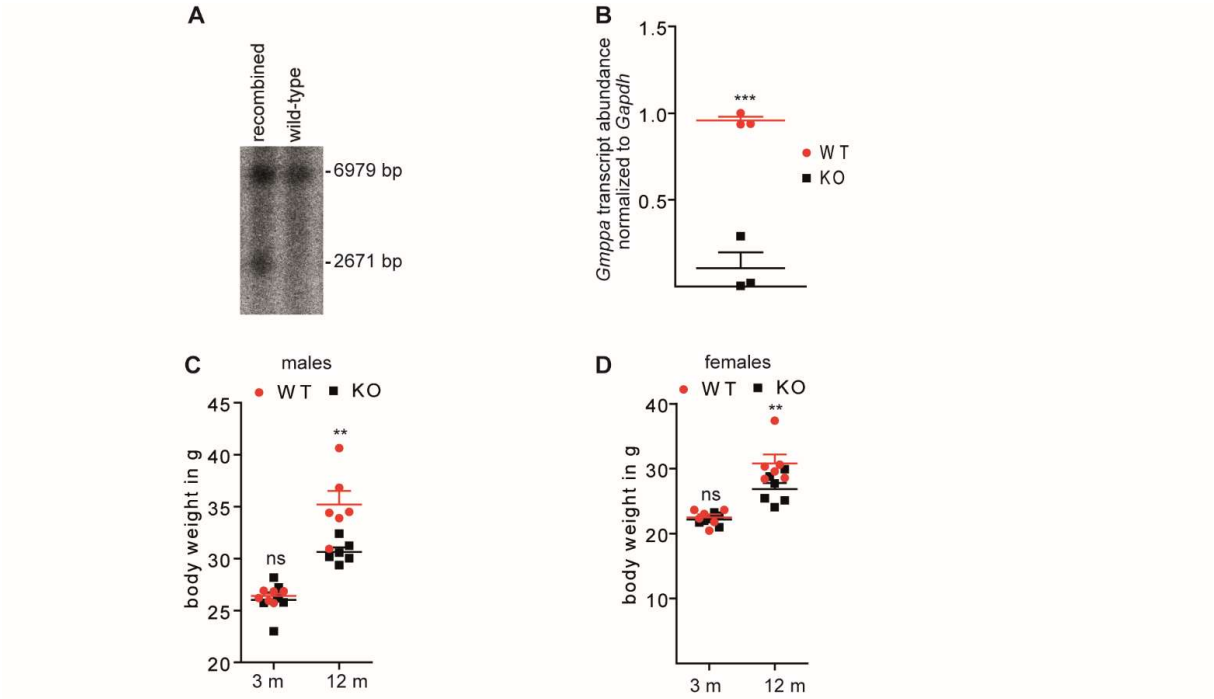


**Supplementary Figure 1. Verification of *Gmppa* KO and body weight of KO mice. A)** Southern blot analysis of the *Gmppa* locus of a WT and a heterozygous KO mouse exploiting the EcoRI restriction sites and the probe displayed in Figure 1A detecting a WT fragment at 6979 bp and a recombined fragment at 2671 bp. **B)** *Gmppa* transcript abundance determined by quantitative RT-PCR is decreased in skeletal muscle lysates of KO mice (n=3 mice per genotype; unpaired 2-tailed Student's t-test). **C,D)** Body weight of 3- and 12-month-old WT and KO mice for C) males and D) females (n=6 mice per genotype and age; 2-way ANOVA with Bonferoni post-hoc test). Quantitative data are presented as mean±SEM and individual data points.

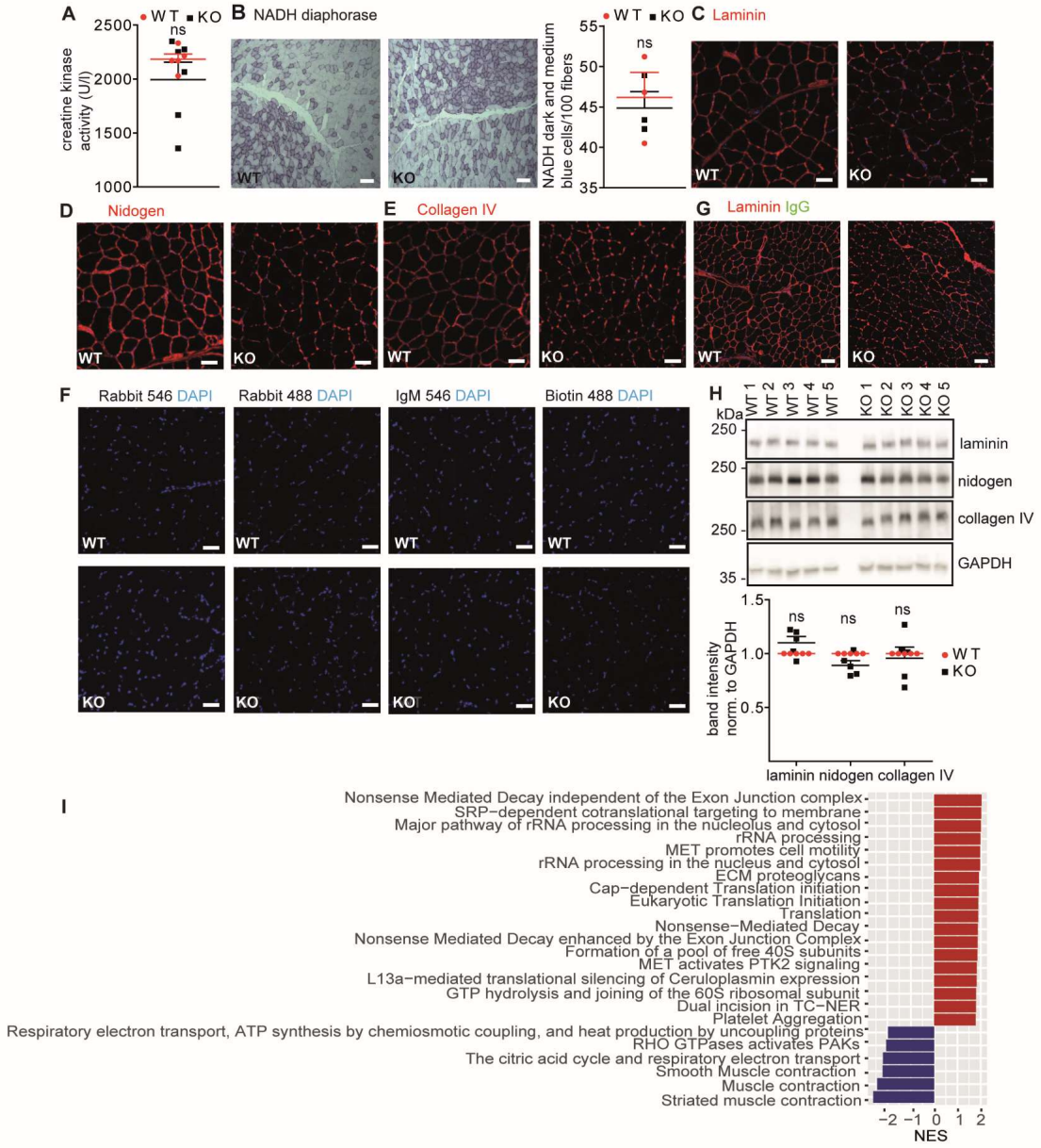


**Supplementary Figure 2. Effect of *Gmppa* disruption on ECM proteins. A)** The creatine kinase activity in the serum of 3-month-old KO mice is not increased (n=3 mice per group; unpaired 2-tailed Student's t-test). **B)** No alteration of the oxidative potential as judged by NADH-diaphorase stainings in 12-month-old KO mice (n=4 mice per group; unpaired 2-tailed Student's t-test; scale bar: 200µm). **C-E)** Lower magnifications of stainings of skeletal muscle sections of 12-month-old WT and KO mice displayed in Figure 2. **C)** Laminin, **D)** Nidogen, **E)** Collagen IV. Scale bars C-E: 50µm. **F)** Control stanings of skeletal muscle sections of 12-month-old WT and KO mice stained with secondary antibodies only and DAPI to label nuclei. Scale bars: 50µm. **G)** The sarcolemma is intact in 12-month-old KO mice as judged by co-staining for laminin and IgG (n=3; scale bars: 100µm). **H)** Nidogen and collagen IV abundances in skeletal muscle lysates are not changed at 12 months of age (n=5 mice each; 2-way ANOVA with Bonferoni post-hoc). GAPDH served as loading control (same membrane as shown in Figure 5C). **I)** Pathway analysis for differentially expressed proteins as determined by mass spectrometry of skeletal muscle lysates of 12-month-old WT and KO mice. Blue indicates down-regulated and red up-regulated pathways in KO mice compared to WT littermates. Data are presented as mean±SEM and individual data points.

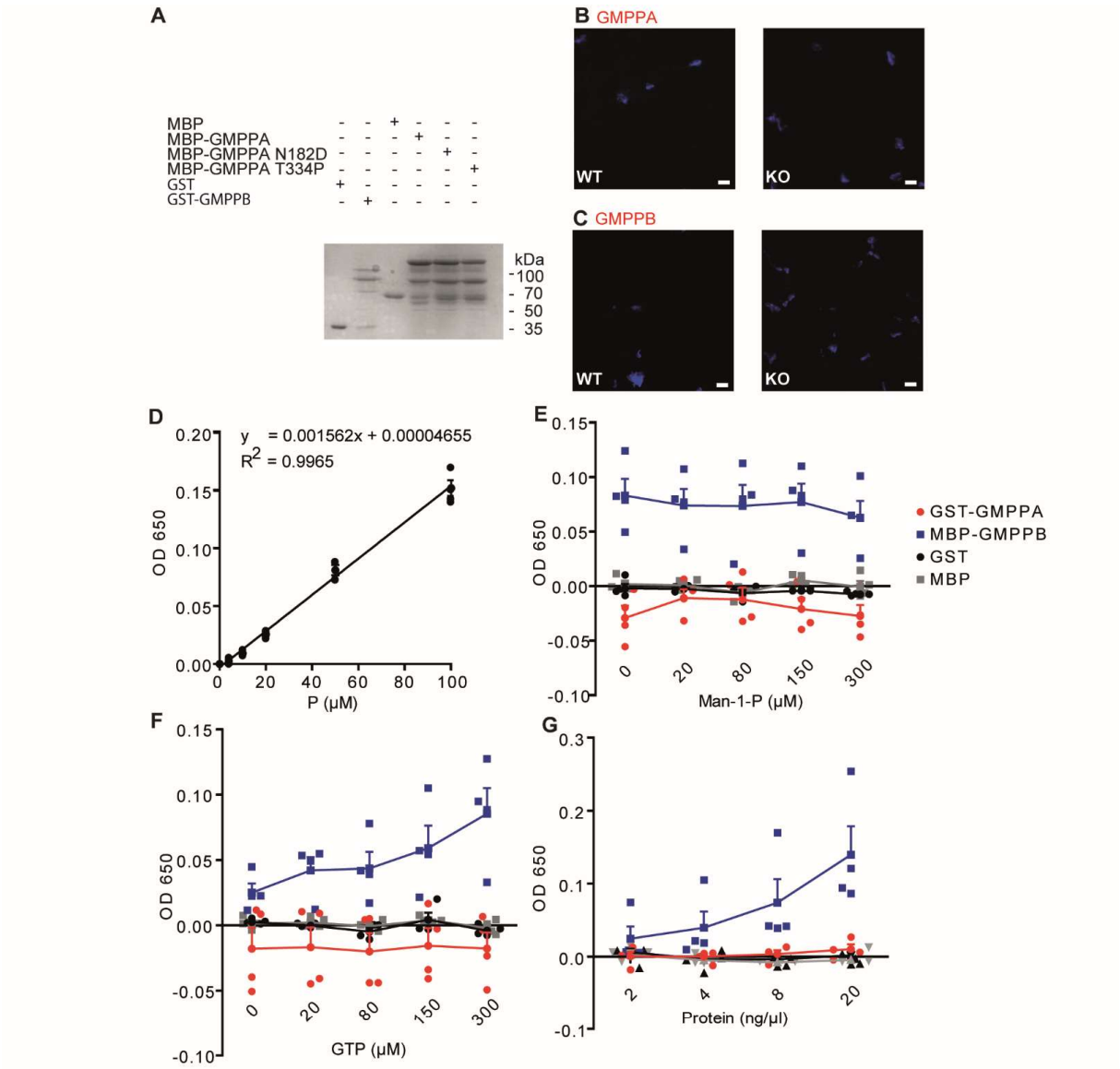


**Supplementary Figure 3. GMPPA is an allosteric inhibitor of GMPPB. A)** Coomassie stained gel of an aliquot of the input for the pull-down assays shown in Figure 4E. **B,C)** PLA assay controls. Scale bars: 5µm. **B)** PLA with skeletal muscle sections from Gmppa WT and KO mice with the GMPPA antibody but without the antibody directed against GMPPB. **C)** PLA assay with skeletal muscle sections from GMPPA WT and KO mice with the GMPPB antibody but without the antibody directed against GMPPA. **D-G)** Control assays for GMPPB and GMPPA activity measurements. **D)** The OD at 650nm is plotted as a function of the phosphate (P) concentration. **E)** Enzyme activities in dependence of mannose-1-phosphate concentrations. **F)** Enzyme activities in dependence of GTP concentrations. **G)** Enzymatic activities in dependence of either GMPPB or GMPPA concentrations. Quantitative data are presented as mean±SEM and individual data points from 4 independent experiments.

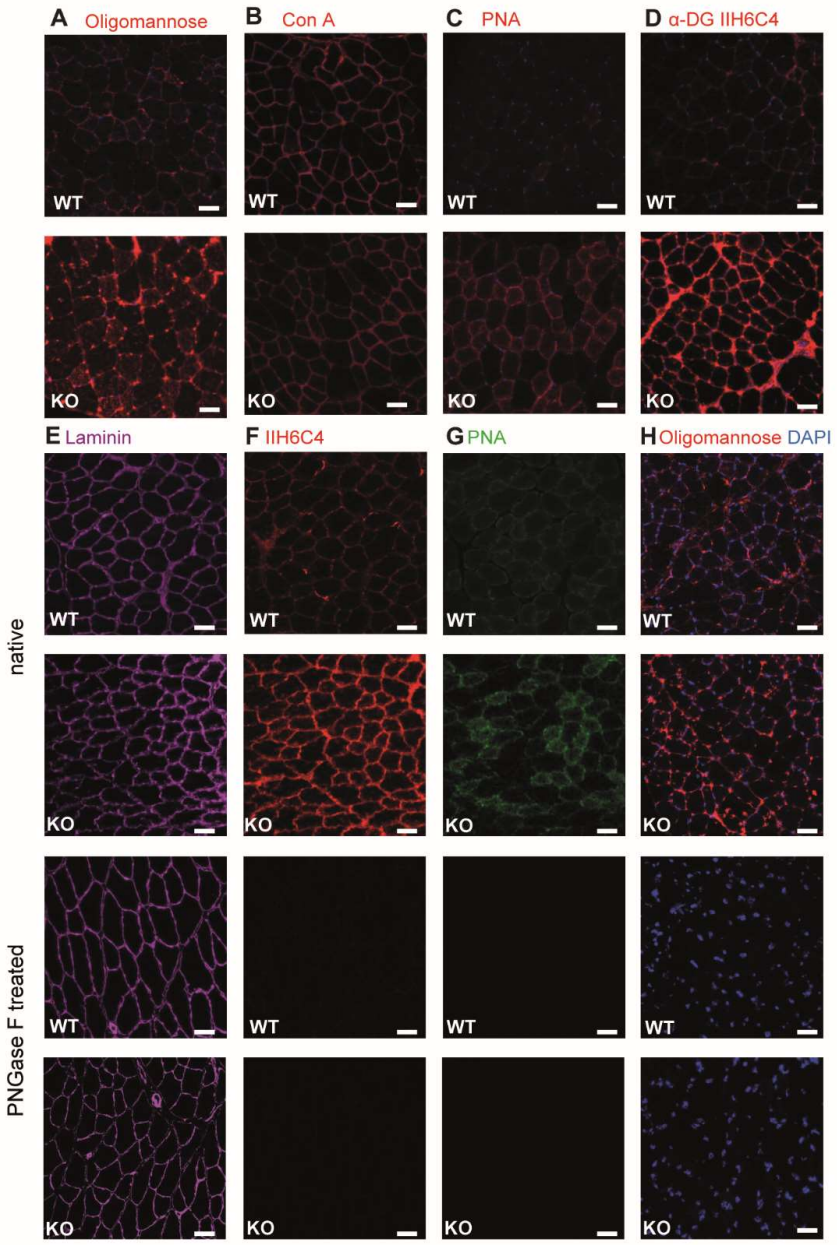


**Supplementary Figure 4. Hyperglycosylation of skeletal muscle proteins in *Gmppa* KO mice.** **A-D)** Lower magnifications of stainings of skeletal muscle sections of 12-month-old WT and KO mice displayed in Figure 5. **A)** Oligomannose, **B)** Con A, **C)** PNA, and **D)** the IIH6C4 antibody directed against the glycosylation specific epitope of α-Dg. Scale bars: 50µm. **E-H)** Stainings of skeletal muscle sections of 12-month-old WT and KO mice with the anibodies/lectins indicated. While signals for oligomannose, PNA, and the glycoslyation-specific epitope of α-DG are absent after prior PNGase F treatment, the signals for laminin are preserved. Scale bars: 50µm.

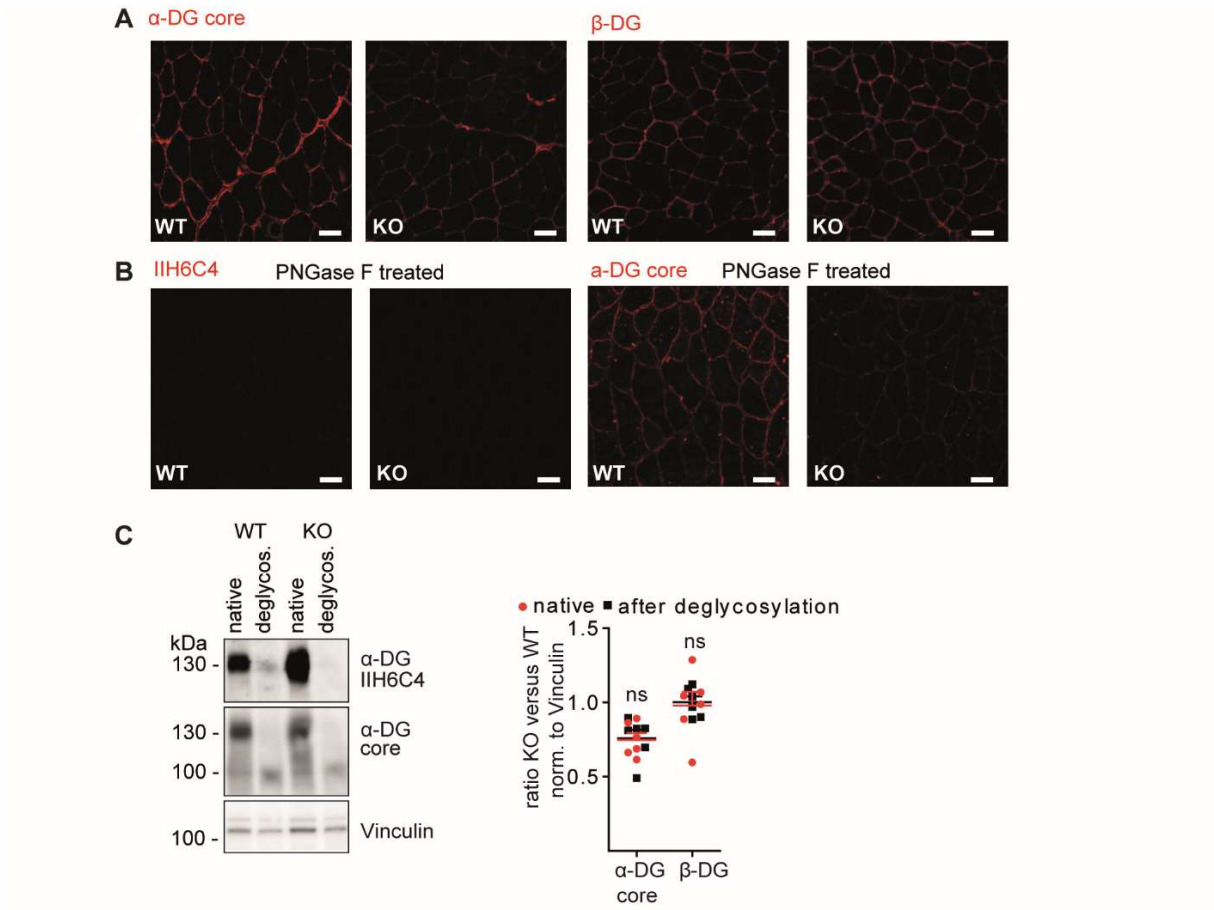


**Supplementary Figure 5. Overviews and control stainings of skeletal muscle sections.** **A)** Lower magnifications of stainings of skeletal muscle sections of 12-month-old WT and KO mice displayed in Figure 7. Scale bars: 50µm. **B)** The α-DG core epitope is not masked by hyperglycosylation. Stainings of skeletal muscle sections of 12-month-old WT and KO mice. While signals for the glycoslyation-specific epitope of α-DG IIH6C4 are absent after PNGase F treatment, signals for the α-DG core protein are preserved. Scale bars: 50µm. **C)** Western blot analysis of protein lysates of skeletal muscle specimen isolated from WT and KO mice with or without deglycosylation (n=5 mice per genotype; 2-way ANOVA with Bonferroni post-hoc test). Data are presented as mean±SEM and individual data points.

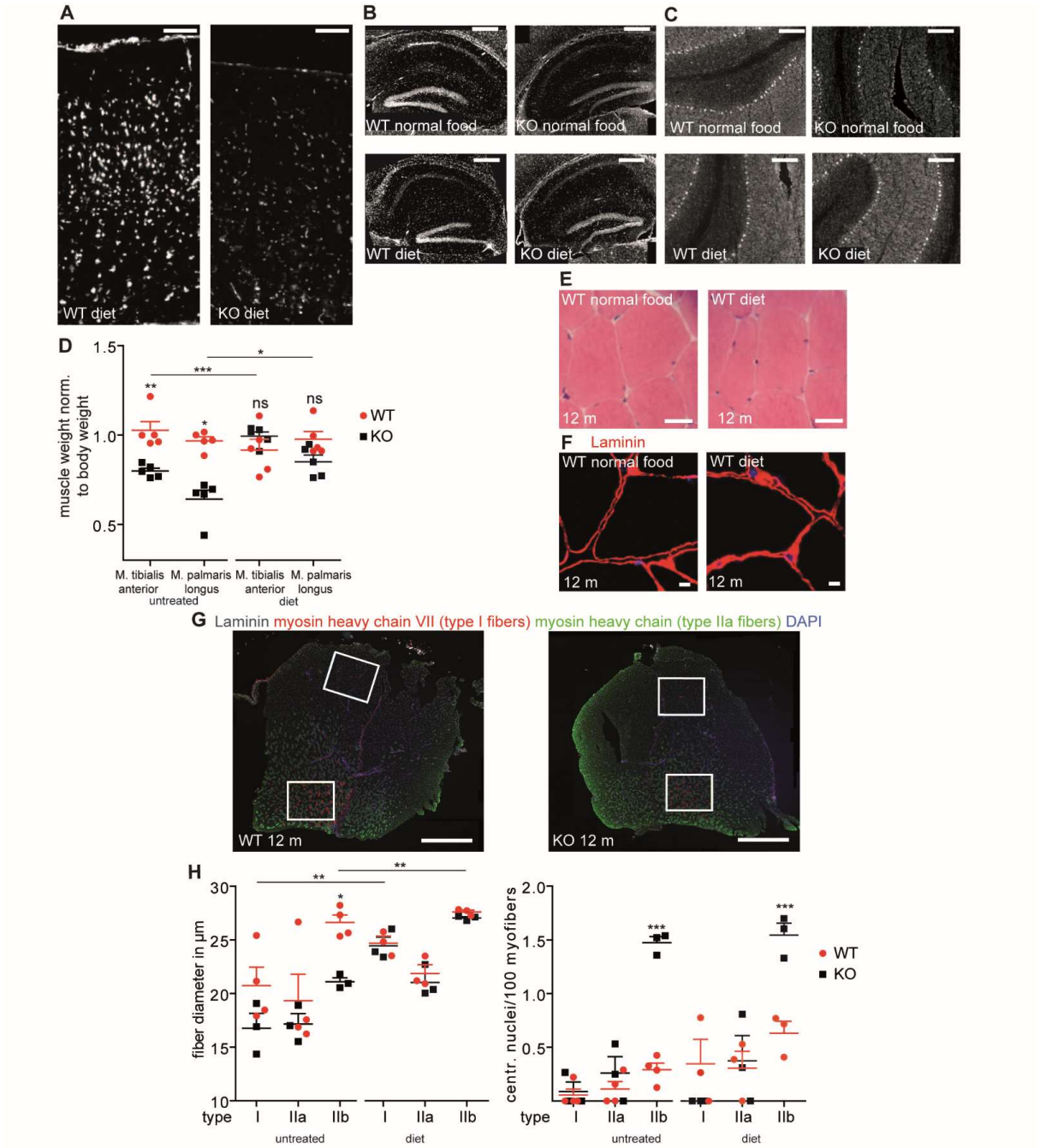


**Supplementary Figure 6. Dietary intervention in WT and KO mice. A)** NeuN stained section of the somatosensory cortex. Scale bars: 50µm. **B)** NeuN stained hippocampal section of an untreated and a treated 12-month-old WT and KO mouse. The quantification is shown in Figure 8. The image for the untreated WT is also displayed in Figure 1. Scale bars: 125µm. **C)** Calbindin-stained cerebellum sections of an untreated and a treated 12-month-old WT and KO mouse. The image for the untreated WT is also displayed in Figure 1. The quantification is shown in Figure 8. Scale bars: 75µm. **D)** Skeletal muscle weight of 12-month-old KO mice either fed on a regular or a nominally mannose-free diet (n=5 mice per group; 2-way ANOVA with Bonferoni post-hoc test). **E)** HE stainings of skeletal muscle sections of WT mice fed on a normal and a mannose-restricted diet. Scale bars: 50µm.The quantification is shown in Fig. 8. **F)** Laminin stainings of skeletal muscle sections of WT mice fed on a normal and a mannose-restricted diet. The quantification is shown in Figure 8. Scale bars: 5µm. **G)** Representative images of the M. gastocnemius/ soleus of 12-month-old WT and KO mice. Areas used for diameter measurements are labeled. Scale bar: 1mm. **H)** Fiber-type specific quantifiction of fiber diameter and centralized nuclei (n=3-5 mice per group; 2-way ANOVA with Bonferoni post-hoc test). Quantitative data are presented as mean±SEM and individual data points.

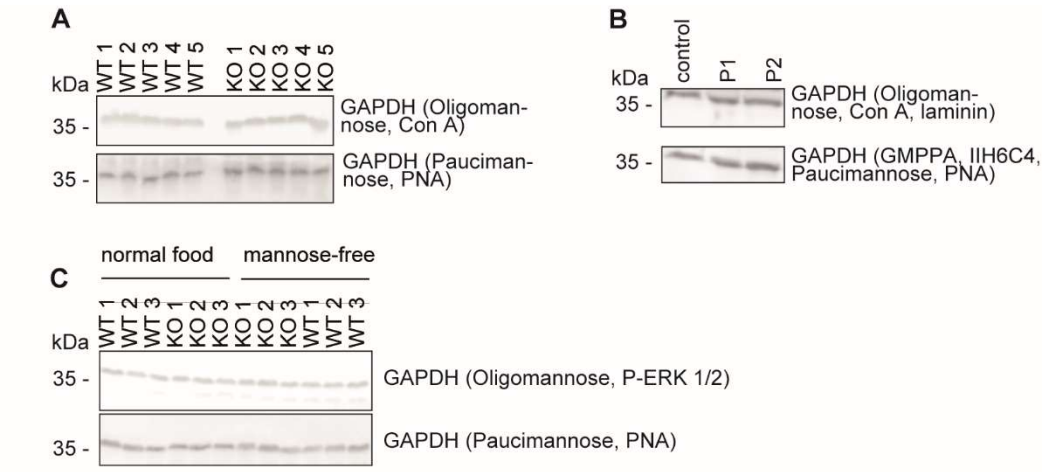


**Supplementary Figure 7. A)** GAPDH loading controls for the membranes displayed in Figure 5. **B)** GAPDH loading controls for the membranes displayed in Figure 7. **C)** GAPDH loading controls for the membranes shown in Figure 8.